

Lifetime of piezoceramic multilayer actuators: Interplay of material properties and actuator design

D.A. van den Ende · B. Bos · W.A. Groen ·
L.M.J.G. Dortmans

Received: 25 July 2007 / Accepted: 27 December 2007 / Published online: 16 January 2008
© Springer Science + Business Media, LLC 2008

Abstract We report an investigation into factors limiting the functional lifetime of multilayer piezoceramic actuators. The study consists of a combination of lifetime experiments by means of an accelerated lifetime test, inspection of the actuator microstructure at different stages of the accelerated lifetime test, and numerical simulation of the displacements and mechanical stresses that arise during actuator performance. During the lifetime test, both displacement and electrical properties were measured. The results show a clear correlation between the microstructure and the mechanical stresses in the actuator, giving evidence that crack initiation starts early in actuator lifetime and humidity effects accelerate degradation. The numerical simulations performed provide clues for optimization of the actuator design with respect to stress development and performance. Attention is paid to the choice of adhesive interlayer and its effect on the performance and lifetime of the actuator.

Keywords Failure analysis · Piezoelectric properties · PZT · Actuators

1 Introduction

A typical multilayer actuator consists of several single thin layer actuators stacked on top of one another; this configuration

has the advantage of achieving large displacements from relatively low applied voltages. These actuators are used for a variety of applications, from nano-positioning stages to active optics controls, to valve actuators [1].

In a general multilayered actuator design there are two regions to be distinguished, an active region and an inactive region [2]. The active region is the region where PZT is surrounded by electrodes and so is submitted to the electric field (see Fig. 1). In this region the PZT will strain upon actuation as a result of the piezoelectric effect [3]. The inactive region is the region of PZT within the stack, which is not between the inner electrodes, so it is never submitted to the electric field. When actuated, the active region induces deformations the inactive regions. The inactive region is then subjected to tensile and bending stresses. In general, cracks will initiate in this region due to these events [2, 4]. Also, the lateral contraction of the active part of the multilayer elements generates shear stresses in the adhesive between the multilayer elements in the stack.

When electrically driven, the PZT material is known to be prone to cracking as a result of strain incompatibilities in the material resulting from its piezoelectric behaviour [5]. Moreover, properties of the actuator containing Ag–Pd electrodes will degrade, due to silver diffusion into the PZT [6, 7, 8]. Furthermore, the degradation is also very much influenced by interactions with water, attracted into the actuator by the electric field [9]. High humidity levels also increase silver migration in the PZT material [10]. This causes material degradation in the active regions, leading to degradation of the actuator as a whole.

In this work, a number of PZT stacks were subjected to an accelerated lifetime test (ALT), during which both displacement and electrical properties were measured, at set intervals. In addition, the actuator microstructure was inspected. Also, numerical simulations of the displacements

D. van den Ende (✉) · B. Bos · L. Dortmans
TNO Science and Industry,
P.O. Box 6235, 5600HE Eindhoven, The Netherlands
e-mail: daan.vandenende@tno.nl

W. Groen
Morgan ElectroCeramics,
Zwaanstraat 2a,
5651 CA Eindhoven, The Netherlands

and mechanical stresses that arise during actuator performance were made, in order to understand the crack growth behaviour and work towards design improvements. A number of effects contribute to the stress states in the actuator, for instance the stiffness of the top layer (added for protection of the active elements), the width of the inactive zones, the stiffness of the surroundings, the application of pre-stress and the stiffness of adhesive layer. One of the design improvements considered in this research was the use of low stiffness adhesives for bonding the different multilayer elements of which the stacks consist.

2 Experimental

2.1 Manufacturing of multilayer stacks

Multilayer PZT elements were obtained from Morgan Electro Ceramics. The elements consisted of 25 of PZT monolayers of 70 μm thickness, fitted with internal electrodes. The width of the inactive layer at the side of the multilayer elements is 0.4 mm and at the top of the elements 0.1 mm. Poled PZT multilayer elements are subjected to an inspection of electric properties (capacitance and insulation resistance) and displacement, prior to assembling them into a stack, which typically consists of 6 multilayer elements. The multilayer elements are adhesively bonded using either an epoxy-based glue or a

silicone-based glue and fitted with two steatite protection layers at the top and bottom. After assembly, a second inspection of the aforementioned electrical properties is performed, before the aforementioned accelerated lifetime test is conducted.

Different stacks were tested under different conditions. The stacks are made of $5 \times 5 \times 2$ mm multilayer elements made of soft PZT material (PG01 material, Morgan Electro Ceramics). The epoxy bonded PG01 stacks were tested at room temperature and 50% RH and at a temperature of 35 $^{\circ}\text{C}$ and a high relative humidity (RH) of 95% RH. A series of PG01 stacks bonded with silicone adhesive was tested at room temperature and 50% RH. The stacks were deliberately not encapsulated to increase the effects of the environment and decrease the lifetime for the purpose of the test. The number of stacks tested per series was set to 10.

2.2 Electrical measurements

As mentioned above, the following electric properties were measured: capacitance and electrical insulation resistance. Capacitance measured with a Precision LCR Meter (Agilent 4284A, 20 Hz–1 MHz) at a low alternating voltage (1 V, 120 Hz). The insulation resistance is the resistance against leakage current. As a large DC voltage is applied to an actuator the insulation resistance will increase due to the charging of the capacitor until a present anomaly makes it possible to conduct current (i.e. a water filled crack or a

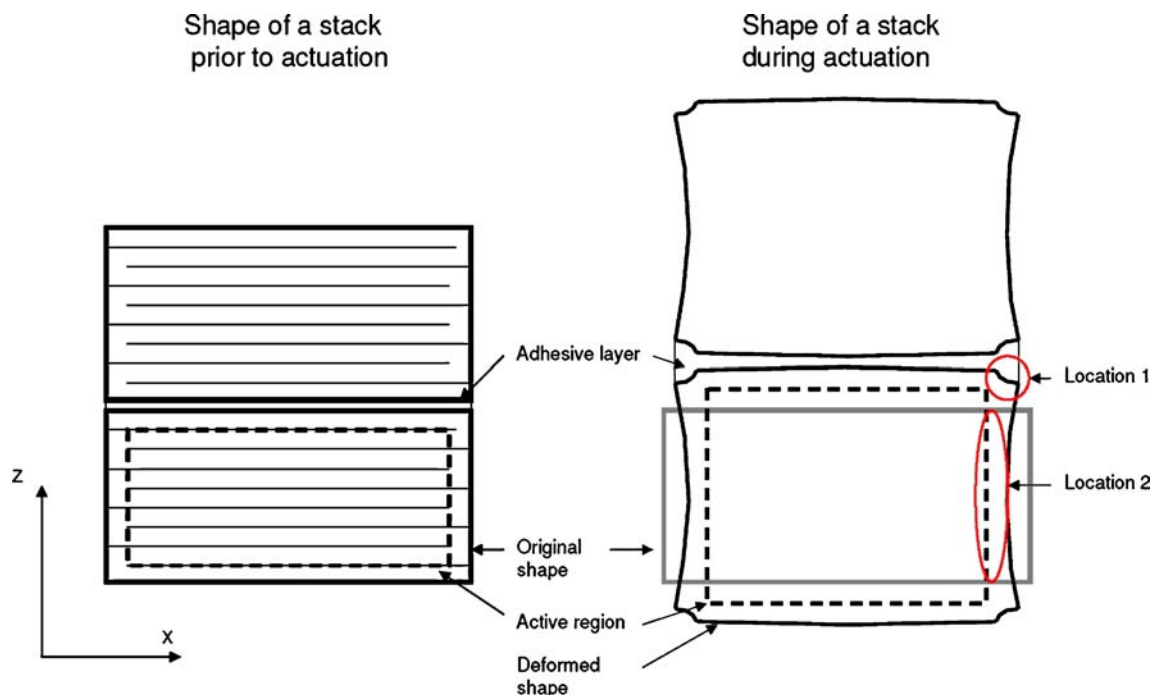


Fig. 1 Schematic representation of a multilayer actuator prior to (*left*) and during (*right*) actuation showing PZT elements and an adhesive layer. Outer corners the PZT elements (*location 1*) and the inner inactive region (*location 2*) are regions where stress concentrations are present

conducting path of silver). As a result the insulation resistance will decrease. The insulation resistance is measured with the Megohmmeter (IM 6, Radiometers A/S) at 216 V (3 V/ μm). The insulation resistance was recorded after 60 s of measurement. Displacement was measured using a linear variable differential transformer (LVDT) at a frequency of 0.1 Hz.

2.3 Accelerated lifetime testing

The purpose of the ALT is to investigate the deterioration of the dielectric properties, displacement and crack formation/growth during a short period of time resembling the behaviour on larger time-scales such as the daily use of sensors and other applications.

During the ALT the stacks are exposed to a block voltage of 150 V (Delta Elektronika SM3004-D) amounting to a cycling field of 2 V/ μm . Using a frequency generator (Philips PM 5127, 10 V) and a switchbox, the stacks were actuated at a frequency of 20 Hz. Functional properties were measured after every decade from 10 to 10⁸ cycles to be able to compare the different trends of deterioration. The output signal of the RC-setting smoothes the block voltage and prevents the stacks from being damaged by the violent change in electric field. In addition resistance multiplied by capacitance (RC) results in a time-constant (t); which is the time-constant for charging of the stack. The resistors must be chosen in such a way ($1/f > RC$) that they allow a stack to fully charge and discharge during the block voltage with a specific frequency to simulate realistic behaviour. In the ALT case, the RC-setting was put at 0.004 s. This is about 10% of the length of the block voltage step and serves to prohibit overshoot in displacement due to abrupt charging of the stack.

2.4 Microstructural inspection

During the ALT a number of samples are removed at set intervals for inspection under an optical microscope. In order to observe the cross sectional features, the samples are polished up to variable depths (0.15, 1.25, 2.5 mm) and inspected using optical microscopy and SEM. Polishing up to 0.15 mm in depth exposes only the inactive region of the PZT stack, whereas polishing up to 1.25 and 2.5 mm exposes the internal electrode structure.

2.5 Numerical modelling

To quantify the expected stresses occurring within a stack a first-order numerical modelling study was performed to understand the stress distributions during actuation and understand the formation of cracks. The model was made up of one steatite protection and three active PZT elements bonded using epoxy or silicone based adhesive.

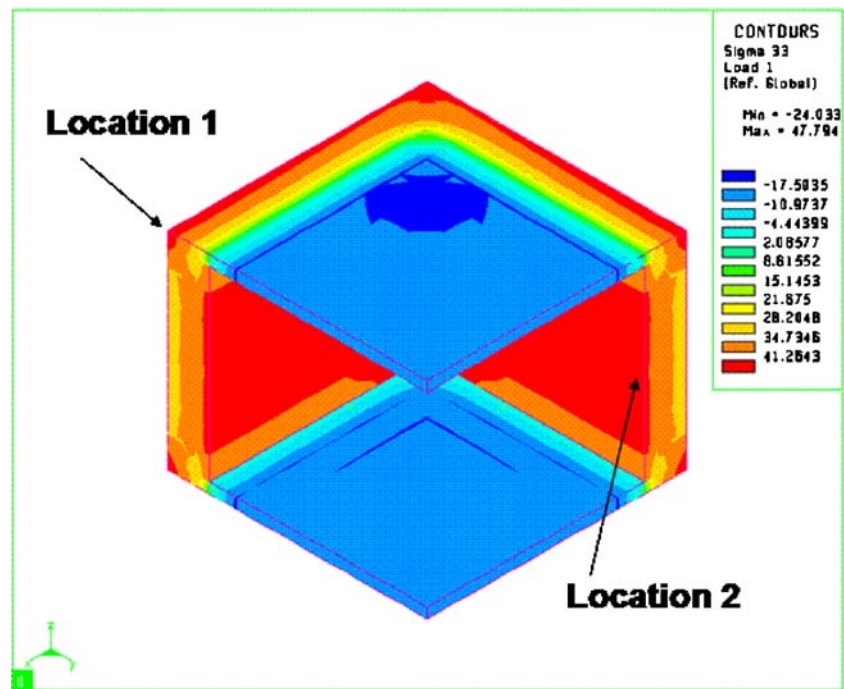
3 Results and discussion

Upon actuation the active part of the multilayer elements expands in the polarization direction, thus contracting in the perpendicular direction, as is visualised in Fig. 1. The protective top layer and the inactive parts of the multilayer elements themselves partly constrain this lateral compression, which leads to shear stresses at this interface (σ_{xz} and σ_{yz}) and tensile stresses in the poling direction in the inactive region near the corners of the upper multilayer PZT element (σ_{zz} at location 1 in Fig. 2). The inactive regions at the sides of the multilayer elements partly constrain the elongation of the active PZT part and tensile stresses in the poling direction (σ_{zz}) arise in this inactive region (σ_{zz} at location 2 in Fig. 2). The presence of shear stresses at the interface between active and inactive regions is evident. This could lead to delamination in the adhesive layers. For this stack geometry, however, no delaminations due to these shear stresses were observed during experiments. A large part of the discussion will be oriented at tensile and bending stresses in the inactive zone (at location 2 in Fig. 1) and the effect of the adhesive layer stiffness on the stresses generated in this zone.

The numerical simulations support this notion. The actuation creates high stress concentrations at the interface of active and inactive regions (i.e. 43 MPa, at location 2 in Fig. 2, for a 5- μm thick epoxy bond). Those stresses (σ_{zz}) initiate cracks parallel to the electrodes (i.e. in the xx or yy directions) at the interface of the active and the inactive regions. High tensile stresses in the poling direction (σ_{zz}) in the stacks are also situated at the corner of the multilayer elements of PZT (i.e. 31 MPa, at location 1 in Fig. 2, for a 5- μm thick epoxy bond). The locations of these stress concentrations are similar to locations found in actuators with a comparable geometry [11]. These stresses lead to cracks starting in the inactive regions of the PZT, running through PZT the multilayer element. Crack initiation was sometimes witnessed during the poling procedure or otherwise during the first few cycles of the ALT. This corresponds to findings in earlier publications [12]. In the case of a silicone based adhesive, the calculated stresses are lowered by at least 25%, as can be seen in Table 1. The silicone adhesive is more compliant than the epoxy. This compliance leads to lower stress states in the inactive regions of the multilayer elements, especially at locations 1 and 2 (see Fig. 2). The results in Table 1 also show that the thickness of the adhesive layer influences the stresses in the PZT elements.

The origin of the stresses at locations 1 and 2, and of the effects of the adhesive stiffness can be understood by thinking of the inactive regions as bars, which are passively deformed when the active region is actuated. This deformation consists of two components: bending due to the

Fig. 2 Stress distribution of stress in zz -direction in one multilayer element in an epoxy bonded actuator (1/4 of element shown). Note tensile stresses of 43 MPa at the inside the inactive region (*location 2*)



inward motion of the sides of the multilayer element and extension in the z -direction because the inactive zones are elongated passively (i.e. dragged along) by the extending active part (as is schematically depicted in Fig. 1). These two components are not independent: the extension tends to straighten the bending bar. The bending component leads to tensile stresses in the poling direction (σ_{zz}) at the inside of the inactive zone and to compressive stresses at the outside (of location 2). The extension in poling direction leads to tensile stress in the poling direction (σ_{zz}) throughout the inactive zone, although it should be noted that this tensile stress is not homogeneous through the thickness of the inactive zone. On the one hand, it is determined by the width of the inactive zone. Also, it is influenced by the stiffness of the glue layer that separates the inactive zones, since the extension in the z -direction upon actuation is distributed between the inactive PZT and the glue. At the upper and lower ends of the inactive zone (i.e. location 1 in Fig. 2) stresses due to the high stiffness of the adhesive layer are

Table 1 Calculated stresses at locations 1 and 2 in the stack for two different adhesives with thicknesses of 5 and 10 μm

Adhesive thickness (μm)	Adhesive stiffness (MPa)	Stress at location 1 (MPa)	Stress at location 2 (MPa)
5	50	3.8	34.1
10	50	1.2	33.3
5	1,800	31.2	42.8
10	1,800	27.1	41.6

highest. Using a low stiffness adhesive leads to much lower stresses at this location, due to the compliance of this adhesive layer.

The effect of adhesive stiffness can now be explained in terms of its effects on the bending- and extensional contributions to the total stresses in the poling direction. Higher adhesive stiffness lowers the relative amount of extension in the adhesive layer between the inactive zones, relative to the extension of the inactive zone itself. Therefore, the amount of extension in the inactive zone itself will increase, and so will the tensile stress in the poling direction (σ_{zz}). This increase applies to the stress on both the outside and the inside of the inactive zone (although not by the same amount). This effect is augmented by the fact that the total displacement of the stack is also higher for a high adhesive stiffness (see Fig. 3). Also, a higher adhesive stiffness reduces the amount of bending in the bar, as the bar is “straightened out” by the stiff adhesive. This will lead to less compression at the outside of the inactive zone, and less tensile stress at the inside. At the outer surface of the inactive zone, the effects of adhesive stiffness on the two effects (bending and extension) complement each other, acting to increase the tensile stresses (σ_{zz}) with increasing adhesive stiffness. At the inner surface of the inactive zone, however, the effect of the adhesive stiffness on the two types of stress work in opposite directions. However, as can be seen from Table 1, at the inner surface of the inactive zone where stresses are the highest, using the low stiffness adhesive does lower the stresses at the inner surface. They are reduced by a significant amount (up to 14.5 MPa for this

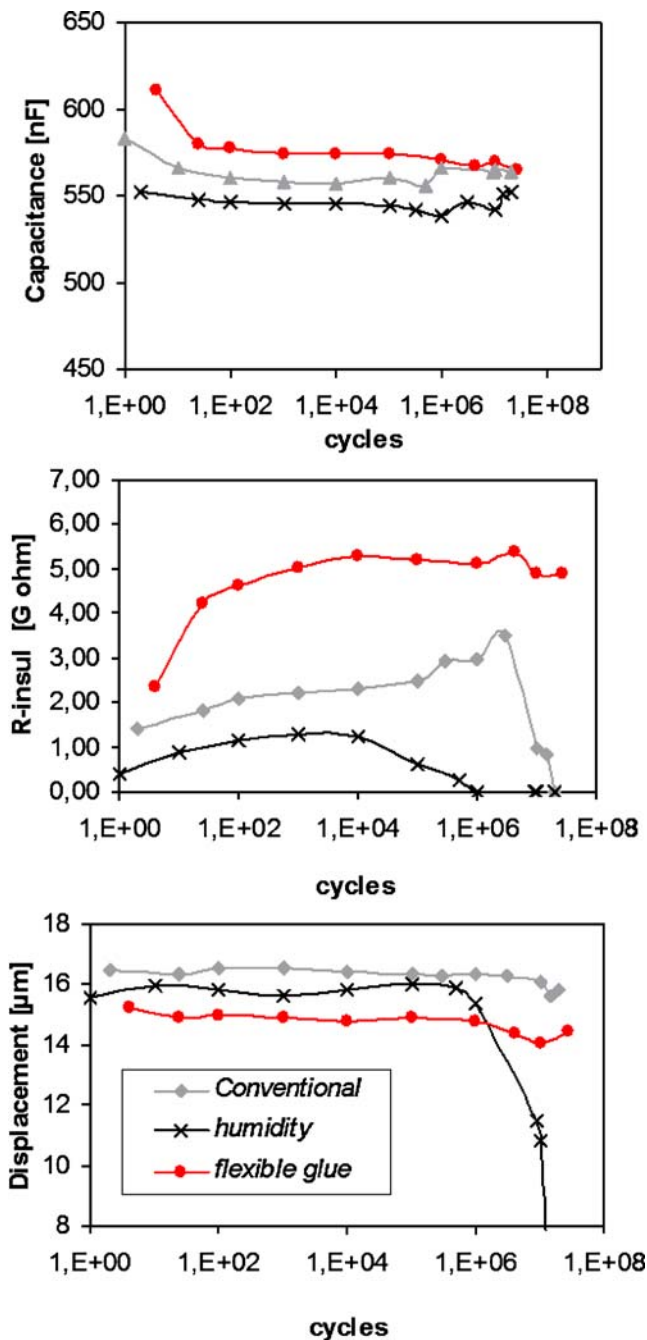


Fig. 3 Typical ALT data: capacitance, insulation resistance and displacement, for PG01 in ambient conditions (conventional), PG01 in a 95% RH environment (humidity) and PG01 with silicone adhesive (flexible glue)

stack configuration). The effect of elongation of the inactive zone is much higher than the straightening of the bending. So using a flexible adhesive will lead to lower stresses in both of the high stress locations (see locations 1 and 2 in Fig. 2 and Table 1). The results of the numerical model are augmented by experimental observations of the microstructure, made during the ALT. In the next section typical ALT results are presented and a correlation of the

stack properties and the microstructure of the stacks is presented.

Typical ALT results are presented in Fig. 3. These results display the capacitance, insulation resistance and displacement of the actuators. These results are the measured average of 10 measured stacks.

3.1 Electrical measurements

Capacitance changes little over the 10⁷ cycles during the ALT. Capacitance primarily depends of the material used for the stack, and also from the degree of poling. The capacitance of a layer may change if a crack is running through this layer, due to the difference in dielectric constant and distance between the electrodes. However, as all layers in the multilayer structure contribute to the total capacitance, the overall measured value is not influenced greatly if one of the ceramic layers is cracked. The results for the insulation resistance of the stacks show an immediate increase in the insulation resistance values. After 10⁴ to 10⁶ cycles the insulation resistance starts to decrease. This could be the result of conducting “through-cracks” in the case of a humid environment (which will be explained in the next section dealing with the microstructure of the stacks). For all cases the decrease in insulation resistance is also the result of silver migration from the internal electrodes, as is mentioned above.

3.2 Displacement

The displacements of the stack actuators do not decrease significantly up to 10⁷ cycles. It has been found that unipolar driven PZT material shows a very small decrease in strain (and therefore displacement of the actuator), even up to 10⁹ cycles [13]. The epoxy bonded stacks tested in a humid environment form the exception. These stacks are completely deteriorated at 10⁷ cycles. This is the result of accelerated crack growth in the humid environment and will be explained below. The displacement of the stack actuators tested shows a higher displacement for the epoxy bonded stacks, than the silicone adhesive bonded stacks. This is because the compliance of the flexible adhesive between the multilayer elements slightly reduces the effectiveness of the piezoelectric actuation.

3.3 Microstructure

In Fig. 4, typical microstructures of PG01 stacks after cycling 10⁷ times, under 2 different conditions are shown. Cracks have formed in the stacks, resulting in the decrease in properties witnessed during the ALT. In this figure only microstructures after 10⁷ cycles are shown. During the test, initial cracks were witnessed after only a few cycles and

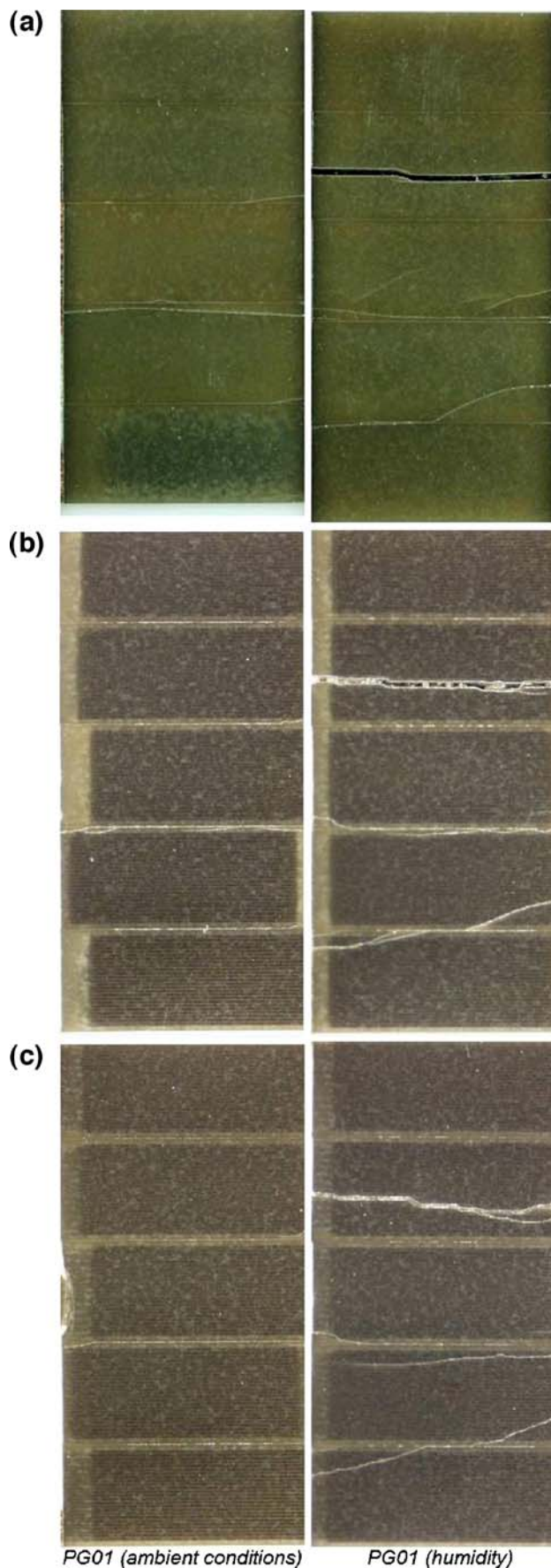


Fig. 4 Cross-sections from stacks as function of depth for 10^7 cycles for PG01 (*left*), and PG01 in a humid environment (*right*). The depths at which the cross-sectional images were taken are: (a) 0.150, (b) 1.125, (c) 2.5 mm

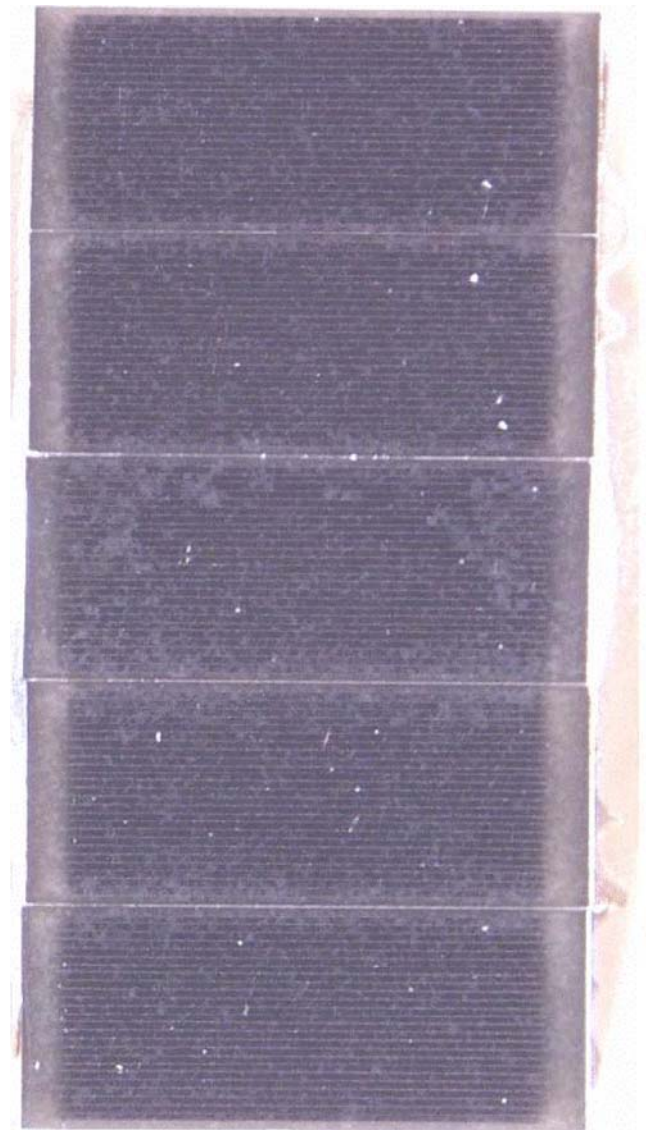
sometimes even directly after poling, in the inactive region of the stack.

The influence of humidity is qualitatively represented by the actuator cross sections in Fig. 4. The actuator tested in a humid environment is cracked more severely than the actuator tested in ambient conditions. The decrease of fracture toughness of PZT with increasing humidity is a cause for this effect [14]. Furthermore the crack propagation is further enhanced due to a concentration of the electric field at the crack tip and subsequent electrolysis of the water present in the crack. The electrolysis of water creates a conducting path in the PZT layer and additionally also degrades the PZT material due to hydrogen charging [9]. This degradation is both electrical (loss in piezoelectric properties) and mechanical (embrittlement). The loss in piezoelectric properties is due to hydrogen atoms in the lattice prohibiting piezoelectric behaviour of the PZT. The loss in mechanical properties leads to accelerated crack propagation. Also migration of the silver already present in the ceramic is enhanced by a high combination of high electric field and humidity levels [10]. This effect is also called electro-migration. This effect is also enhanced by the existence of cracks in the actuator as a concentration of electric field strength at the crack tip exists. This correlates to the electrical and displacement measurements, where the losses in both insulation resistance and displacement are much more severe for the humidity tests.

When using silicone as an adhesive, the crack formation during the ALT is much less severe (see Fig. 5). The stress concentrations in the stack (especially at locations 1 and 2 of Fig. 2) are limited (see Table 1) and as a result, crack formation is limited too.

In general, cracks will lead to an initial increase in resistance, as the growing cracks will interrupt the electrical paths between electrodes. However the high insulation resistance of the stacks bonded with the flexible silicone based adhesive, which poses much less cracks as is explained below, contradict this hypothesis. This can be a result of cracks running through the epoxy layer itself, thereby effectively connecting the electrodes on the edges of the stacks, whereas with silicone adhesive, these cracks do not exist, as can be seen in Figs. 4 and 5. In general the insulation resistance will eventually decrease, either when silver migration decreases resistivity in the PZT layers, or when crack growth reaches a stadium where electrically conducting paths are close to forming through the whole stack. The speed at which this happens is dependent on the humidity of the environment. The electrolysis of water

Fig. 5 Cross-sections from stacks as function of depth for 10^7 cycles for PG01 bonded with flexible silicone adhesive at a depth of 1.125 mm



PG01 prepared with silicone adhesive

which has penetrated into the cracks is suspected lead to faster deterioration of the resistance. This does not however, immediately lead to a decrease in displacement. Only after a great number of cycles the displacement decreases rapidly (for humid environments). The reason for this is the existence of a conducting through crack, connecting both side electrodes, in a number of these samples. This explains why the stack tested in a humid environment degrades faster than stacks tested under ambient conditions, which show little loss in displacement up to 10^7 cycles. However, the loss in insulation resistance witnessed in these stacks, does in fact predict that the end of the functional lifetime is also imminent for these stacks. The research shows that one way to increase functional lifetime is the use of a flexible adhesive during assembly of the stacks. The stacks bonded with silicone adhesive do not

have such a large actuation displacement as the epoxy bonded stacks. However, the decrease in actuation strain is no more than 10% and leaves the strain of the components inside specifications for the target applications. This slight loss is more than compensated by the increase in lifetime for certain low frequency applications. It must be noted here that the possibilities for use when using pre-stressed stacks or high frequency actuation can be limited, due to the low stiffness of the silicone adhesive. These conditions were not tested in this research.

4 Conclusions

In accelerated lifetime testing of the PG01 stacks, correlations between crack locations in experiments and stress

concentrations in numerical simulations are evident. The lifetime tests indicate that cracks originate in the inactive regions of the stack, after a small number of cycles or even during poling. The losses in insulation resistance occur prior to the losses in displacement in all samples. The insulation resistance decreases before 10^7 cycles while the displacement is largely unaffected up until 10^7 cycles. The effect of through cracks correlate these losses in functional properties to the microstructure of the stacks. The use of flexible silicone based adhesive in stack assembly is one of the methods available to reduce stress concentrations in the inactive region of the PZT material, as is indicated by numerical simulations. This statement is supported by the experiments since no cracks are present in material prepared with flexible silicone based adhesive, whereas the epoxy bonded specimens suffered severed cracking during an accelerated lifetime test, thereby complementing results of the FEM model. However, the use of a flexible adhesive will reduce displacement of the actuator slightly. However, this slight loss is compensated by the increase in actuator lifetime. The stiffness of the stack is also reduced and care must be taken in high frequency applications.

References

1. F. Claeysen, R. Le Letty, in *Piezoelectric Materials in Devices*, ed. by N. Setter (EPFL 2002), p. 103
2. K. Lubitz, C. Schuh, T. Steinkopff, A. Wolff, in *Piezoelectric Materials in Devices*, ed. by N. Setter (EPFL 2002), p. 183
3. S.J. Jeong, M.S. Ha, J.S. Song, *Sens. Actuators, A, Phys* **116**, 509 (2004)
4. S.L. dos Santos e Lucato, D.C. Lupascu, J. Rödel, *J. Eur. Ceram. Soc* **21**, 1425 (2001)
5. S.L. dos Santos e Lucato, H.A. Bahr, V.B. Pham, D.C. Lupascu, H. Balke, J. Rödel, U. Bahr, *J. Mech. Phys. Solids* **50**, 2333 (2002)
6. S. Yoshikawa, M. Farrell, *SPIE* **3985**, 652 (2000)
7. M.V. Slinkina, G.I. Dontzov, V.M. Zhukovsky, *J. Mater. Sci* **28**, 5189 (1993)
8. L.J. Ecclestone, I.M. Reaney, W.E. Lee, *J. Eur. Ceram. Soc* **25**, 1647 (2005)
9. X.P. Jiang, W.P. Chen, Z. Peng, M. Zeng, H.L.W. Chan, C.L. Choy, Q.R. Yin, *Ceram. Int* **32**, 583 (2006)
10. J.C. Lin, J.-Y. Chan, *Mater. Chem. Phys* **43**, 256 (1996)
11. D. Borza, D. Lemosse, E. Pagnacco, *Compos. Struct* **82**, 36 (2008)
12. G.A. Schneider, H. Weitzing, B. Zickgraf, *Fract. Mech. Ceram* **12**, 149 (1996)
13. C. Verdier, D.C. Lupascu, J. Rödel, *J. Eur. Ceram. Soc* **23**, 1409 (2003)
14. N. van der Laag, Ph.D. Thesis, TUE, Eindhoven (2002)